

Abbas SOLTANI <sup>1</sup>, Milad ARIANFARD<sup>2</sup>, Reza Nakhaie JAZAR <sup>3</sup>

## Application of unscented Kalman filter for clutch position control of automated manual transmission

Received 25 October 2021, Revised 1 February 2022, Accepted 16 February 2022, Published online 22 April 2022

**Keywords:** automated clutch, actuator, adaptive sliding mode control, estimator, unscented Kalman filter

In this paper, an adaptive sliding mode controller (ASMC) is proposed for an electromechanical clutch position control system to apply in the automated manual transmission. Transmission systems undergo changes in parameters with respect to the wide range of driving condition, such as changing in friction coefficient of clutch disc and stiffness of diaphragm spring, hence, an adaptive robust control method is required to guarantee system stability and overcome the uncertainties and disturbances. As the majority of transmission dynamics variables cannot be measured in a cost-efficient way, a non-linear estimator based on unscented Kalman filter (UKF) is designed to estimate the state variables of the system. Also, a non-linear dynamic model of the electromechanical actuator is presented for the automated clutch system. The model is validated with experimental test results. Numerical simulation of a reference input for clutch bearing displacement is performed in computer simulation to evaluate the performance of controller and estimator. The results demonstrate the high effectiveness of the proposed controller against the conventional sliding mode controller to track precisely the desired trajectories.

### 1. Introduction

Nowadays, the two types of most widely utilized transmission systems are manual transmission (MT) and automatic transmission (AT), each with their advantages and disadvantages. With the development of electronics and intelligent

✉ Abbas SOLTANI, e-mail: [soltani@bzte.ac.ir](mailto:soltani@bzte.ac.ir)

<sup>1</sup>Buin Zahra Higher Education Centre of Engineering and Technology, Imam Khomeini International University, Qazvin, Iran. ORCID: 0000-0001-5764-7591

<sup>2</sup>Department of Mechanical Engineering, Technical and Vocational University (TVU), Tehran, Iran

<sup>3</sup>School of Mechanical and Automotive Engineering, RMIT University, Melbourne, Australia. ORCID: 0000-0003-2534-980X



© 2022. The Author(s). This is an open-access article distributed under the terms of the Creative Commons Attribution-NonCommercial-NoDerivatives License (CC BY-NC-ND 4.0, <https://creativecommons.org/licenses/by-nc-nd/4.0/>), which permits use, distribution, and reproduction in any medium, provided that the Article is properly cited, the use is non-commercial, and no modifications or adaptations are made.

systems and their application in mechatronic systems of the vehicles, the idea of automating the MT using actuators and intelligent controllers was introduced as an automated manual transmission (AMT).

The control of the clutch motion will affect the engine speed and the angular clutch velocity during the clutch engagement, so that if the controller is not well designed, it can cause fluctuations and vibrations in the power transmission system and as a result, the driver will not enjoy comfort. Clutch actuation is one of the most complex stages of the AMT. The automated clutch can be disengaged and engaged automatically and should be designed to satisfy different and conflicting objectives such as small friction losses, minimum time required for the engagement, and driver comfort during the engaging and disengaging process [1]. A control method was developed to track the reference clutch torque to achieve the desirable performance. The clutch torque control has been proposed based on the engine and clutch reference velocities [2].

Hydraulic and electrohydraulic actuators are still applied for the automation control of AMT. Nowadays, the electromechanical actuator is taken into account as an alternative solution, as it improves the transmission efficiency and dynamic response. Recent attempts employ the electromechanical actuators utilizing the DC motors in conjunction with reduction gear to achieve the desired driving force. In order to improve the AMT performance, a large number of articles about electromechanical actuators have been published recently. In reference [3], DC motors were used to replace the gearshift lever, and a new gear selector combined with cables was presented. A new methodology for the electromechanical clutch position control systems was proposed. A non-linear dynamic model for the screw-nut actuator associated with a clutch was introduced, and then a dynamic SMC with fuzzy adaptive tuning was designed [4]. A dynamic model for the hydraulic clutch actuator was utilized in the actual transmissions. To evaluate the operation characteristics of the AMT system, a control approach to ensure desirable performance was investigated. The gearshift control logic and the PID-based clutch control were presented [5].

A new gearshift system was designed applying a 2-DOF electromagnetic actuator to realize the automation of gearshift [6]. Position tracking control was implemented for the motor-driven gear-shift actuating mechanism of the electromechanical AMT system. To realize rapid and precise gear-shift control, an optimal discrete-time preview position control scheme was introduced [7]. Chyuan-Yow et al. proposed an electric vehicle by developing a dynamic model of the clutchless AMT driveline [8]. A new hybrid optimal algorithm for the DC motor of electromechanical AMT was designed. It included a non-linear time optimal controller and optimal linear quadratic regulator [9]. Oh et al. developed a tracking controller for the self-energizing clutch actuator system consisting of a DC motor and an encoder for the AMT [10].

In most previous research, the state variables of the AMT system were considered measurable. Since some state variables like rotational speed and acceleration of the clutch actuator and the drive shaft torque cannot be measured in a cost-efficient way, considerable errors can occur in the performance of the AMT control system. As a result, a state estimator is required to guarantee the accuracy and robustness of the controller. In this regard, a Kalman filtering was adopted to estimate the states of vehicle stability control systems such as the longitudinal and lateral vehicle velocities and the slip ratio of tires [11]. Gao and et al. designed a clutch disengagement strategy to control the AMT. The control methodology was based on design of an observer to estimate the drive shaft torque [12].

Due to hard non-linearity of the spring stiffness of the actuator and clutch, a nonlinear estimator is needed to estimate the system states. To achieve this, many approaches have been suggested such as recursive least-square, sliding mode observer, EKF and UKF. However, the EKF has been rarely investigated in the previous AMT studies. When an EKF is applied to a complex non-linear system, a few problems may arise. One of them is the computation of the state transition matrix which requires the calculation of the Jacobian matrix. Moreover, the linearization can make large errors and even cause divergence of the filter. To overcome this limitation, the UKF is utilized and developed currently. The UKF algorithm has many advantages over the EKF, especially in case of high non-linearity. The UKF directly uses nonlinear equations of the system and does not require the linearization [11].

A SMC was proposed to design the combined electromechanical and electrohydraulic actuators. The main focus of this study was on pressure control in an electrohydraulic actuator with time-varying parameters without using the observer of state variables and the clutch spring was modeled nonlinearly [13]. In another paper, the researchers proposed a combination of a proportional-integral-derivative controller and a SMC to design an electromechanical actuator control system. However, the effect of parametric uncertainties on the controller performance was not investigated and the state variables used in the design of the control system were measurable. As a result, the estimator was not adopted in the control algorithm [14].

Recently, an optimization method of reference clutch slip speed in clutch slip engagement in the vehicle powertrain has been proposed to improve clutch lifespan and vehicle ride comfort. The presented method was verified through clutch slip engagement simulations using AMESIM and MATLAB Simulink [15]. A novel hybrid optimal algorithm for the DC motor of electro-mechanical AMT was developed. It combined non-linear time optimal controller and optimal linear quadratic regulator consequently used at different shifting stages. The working principle, dynamic characteristics of the AMT system and the model of the DC motor were presented [9].

To eliminate or reduce torque interruption and driveline jerk during clutch engagement for AMT systems, a gearshift assistant mechanism was designed. The

proposed mechanism consisted of a torque complementary motor and an epicyclic mechanism with a synchronizing clutch. During gear upshift, the electrical motor provided complementary torque to the output shaft after synchronizer discharges, then the synchronizing clutch worked to synchronize output shaft [16]. A clutch control strategy was proposed to improve the shift quality of power shift transmission and solve the power cycle phenomenon in the shifting process. The analysis of change in the transmission torque and the relationship between the rotating speed of the driving and driven disks of a shifting clutch was carried out. Simulations and experiments were performed on the optimization results based on particle swarm method [17]. Also, a new methodology for online identification of the dry-clutch torque characteristics model in vehicular transmission systems was developed. The proposed approach provided a tool with capability to estimate the clutch torque model parameters directly, using the measurable signals of engine torque and speed within a multiple model predictive control loop, in real time. The calculation of the clutch torque with uncertainties was presented [18].

According to the review of presented studies, the main contribution of this paper is a combined use of ASMC and UKF estimator to improve the clutch position control performance for the AMT system. The designed ASMC, which is insensitive to system uncertainties, offers the adaptive sliding gains to eliminate the bounds of uncertainties. The rotational speed and acceleration of the clutch actuator are estimated in real time utilizing the UKF. A non-linear dynamic model of the electromechanical clutch actuator is constructed precisely and validated with experimental test results.

The rest of the paper is organized as follows. In the Section 2 of the article, a nonlinear electromechanical actuator model for the clutch system is explained. Then, the validation of actuator model is presented based on experimental test results. In the Section 3, the design of a state estimator using the UKF is discussed. The clutch position control methodology is proposed through the ASMC in the Section 4. The performance of the designed clutch controller is investigated with several simulations in the Section 5. Finally, the conclusions are listed and discussed.

## 2. Electromechanical clutch actuator model

The electromechanical clutch actuator model uses an electric motor to engage and disengage the clutch. In the clutch actuator, the rotary movement of the electric motor is transferred via a toothed gear segment into a linear movement, which is then used to open the clutch with the help of the release lever and release bearing. The clutch actuator is shown in Fig. 1. The clutch actuator is composed of a permanent-magnet DC motor, a set of pinion and gear, coil spring and slider crank mechanism.



Fig. 1. The clutch actuator

## 2.1. Electric motor model

In this section, the armature-current controlled DC motor model is presented for controller design. In the armature current control, only the voltage applied to the armature of the motor is adjusted. Fig. 2 shows the DC motor equivalent model for clutch actuator. Based on the electrical system equation and the mechanical system equation, the mathematical model of the electromechanical system can be described as follows [19]:

$$L_a \frac{di_a}{dt} + R_a i_a + k_e \omega_m = u_a, \quad (1)$$

$$J_m \frac{d\omega_m}{dt} + B_m \omega_m = k_t i_a - T_L, \quad (2)$$

where the states are the angular speed  $\omega_m$  of the motor and the armature current  $i_a$ ,  $u_a$  represents the voltage of the DC supply source,  $T_L$  is the load torque considered as a disturbance,  $B_m$  is the viscous friction coefficient,  $J_m$  is the moment of inertia,  $k_t$  is the electromechanical coupling coefficient,  $k_e$  is the back electromotive force (e.m.f) constant,  $R_a$  is the armature resistance, and  $L_a$  is the armature inductance.

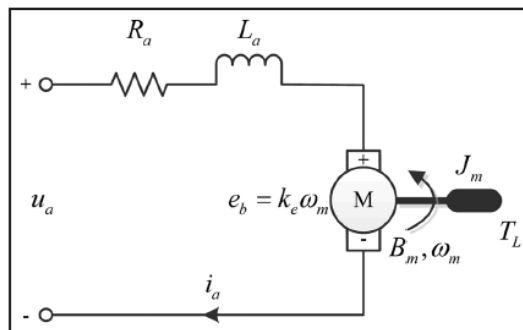


Fig. 2. An equivalent model of the clutch actuator motor

## 2.2. Actuator mechanism model

A schematic diagram of the clutch actuating mechanism is shown in Fig. 3. As shown in the figure, the system mainly consists of three components: a gear, a coil spring and a slider crank mechanism. Thus, the system model is obtained by a set of kinematics and kinetics equations which describes the dynamics of the electromechanical actuator. The slider crank includes links of BC and AB and revolute joints A, B and C. The points of C and F are fixed and point A has translation motion. Therefore, the length of the straight-line  $\overline{CF}$ , which represents the distance from point C to point F, is constant. The F and E points are the beginning and end points of the coil spring. Since the gear is a rigid body and points C and E are two points on the gear, the distance between them,  $\overline{CE}$ , will be constant. Although, point E is a moving point due to the rotation of the gear.

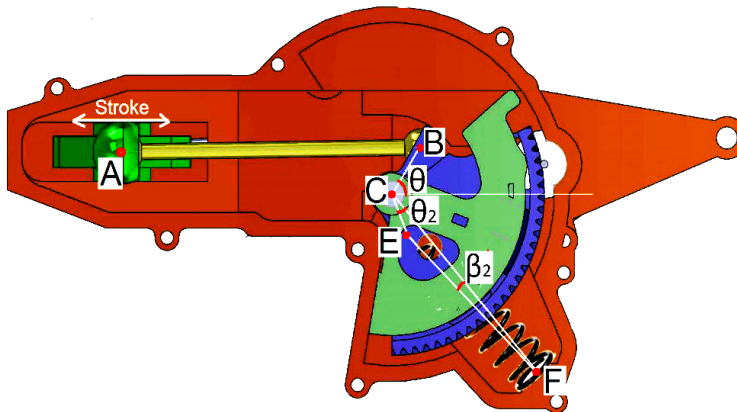


Fig. 3. Schematic diagram of the clutch actuating mechanism

### 2.2.1. Kinematics actuator mechanism model

The input gear link is a compound member with a circular segment. There are teeth around this link that engage the electromotor pinion. Angular velocity of the gear is  $\omega = \dot{\theta}$ . According to the geometry of mechanism, trigonometric relations and, also the relative motion analysis, derivative of the spring length is obtained as follows:

$$\dot{\overline{EF}} = \frac{\overline{CE} \cdot \overline{CF} \cdot \omega \sin \theta_2}{\overline{EF}} = \frac{17.665 \times 10^{-4} \omega \sin \theta_2}{\overline{EF}} \quad (3)$$

The length of spring is calculated by solving the differential Eq. (3) with initial condition  $\overline{EF}_0 = 45.7$  mm. So, the spring force and its torque around point E

is determined if angle  $\beta_2$  is known. This angle is found as follows with initial condition  $\beta_2 = 1.18^\circ$ :

$$\dot{\beta}_2 = \frac{-\overline{CE} \cdot \omega \cos(\theta_2 + \beta_2)}{\overline{EF}} = \frac{-0.025\omega \cos(\theta_2 + \beta_2)}{\overline{EF}}. \quad (4)$$

### 2.2.2. Kinetics actuator mechanism model

First, it is necessary to obtain the nonlinear equation of the diaphragm spring force,  $F_s$  for clutch in terms of its deflection ( $x_c$ ). Laboratory test data were used for this. To determine the equation, a clutch spring was tested by a tensile pressure tester. For this purpose, a clutch with a diaphragm spring was compressed at room temperature. The force and displacement values were measured by a dynamometer with an accuracy of 0.1 N and a capacity of 150 kN and an encoder with an accuracy of 0.001 mm, respectively. Using MATLAB software, a fourth-order polynomial in terms of  $x$  displacement can be approximated as:

$$F_s = 5.91 \times 10^{11} x_c^4 - 8.3 \times 10^9 x_c^3 + 2.344 \times 10^6 x_c^2 + 3.065 \times 10^5 x_c - 17.68. \quad (5)$$

The load–deflection curve for the diaphragm spring of the clutch is plotted in Fig. 4. In this figure, slight deviation from the test result is observed at 0.008 m, but it is not so significant. Because the clutch is completely disengaged in this zone. Trying to perfectly curve fitting in the region causes the curvature to deviate around the point of maximum. Since these areas are more important to control the clutch, it makes undesired performance of the controller.

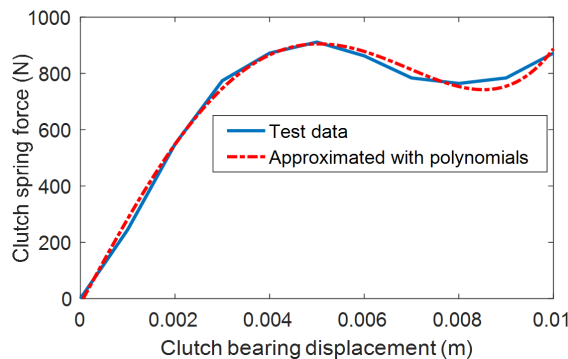


Fig. 4. Load–deflection curve for the diaphragm spring

The equations of motion may be written utilizing Lagrange equation. The gear ratio between the input gear link and electromotor pinion is  $N_m = 40.5$ . The input torque of actuator is obtained through multiplying this value by the electromotor

torque. The relation between the clutch bearing displacement  $x_c$  in terms of  $\theta$  can be derived as:

$$x_c = c_1\theta - c_2, \quad c_1 = 0.0062, \quad c_2 = 0.0063. \quad (6)$$

The total torque of the coil spring and the clutch diaphragm spring is considered as the load torque  $T_L$ . The state variables are given as:

$$X = [x_1 \ x_2]^T = [\omega \ \dot{\omega}]^T. \quad (7)$$

According to the mentioned dynamic equations of clutch actuator, the state equations are given by:

$$\dot{x}_1 = x_2 = \dot{\omega}, \quad (8)$$

$$\begin{aligned} \dot{x}_2 = \ddot{\omega} = & \left(\frac{1}{I_a}\right) \left[ -\left(k_\omega + \frac{R_a I_a}{L_a}\right) x_2 - \left(\frac{R_a k_\omega + k_t N_m^2 k_e}{L_a}\right) x_1 \right. \\ & \left. + \left(\frac{R_a T_L}{L_a}\right) + \dot{T}_L + \left(\frac{k_t N_m}{L_a}\right) u_a \right], \end{aligned} \quad (9)$$

$$T_L = -0.906\theta^3 - 4.94\theta^2 + 28.68\theta - 25.03, \quad (10)$$

where  $I_a = 0.02 \text{ kg m}^2$  represents the moment of inertia of the entire system,  $\ddot{\omega} = \dot{\alpha}$  is derivative of angular acceleration and  $k_\omega = 0.32$ . The system output equation is expressed as:

$$y = [y_1 \ y_2]^T = [\theta \ i_a]^T, \quad (11)$$

$$y_1 = \theta = \int \omega dt = \int x_1 dt, \quad (12)$$

$$y_2 = i_a = \left(\frac{I_a x_2 + k_\omega x_1 - T_L}{k_t N_m}\right). \quad (13)$$

### 2.2.3. Model validation

After actuator modelling, several tests run to investigate performance of the clutch actuator which is driven by the DC electromotor with the  $u_a = 14 \text{ V}$  rated voltages. In these tests, the clutch actuator is mounted on clutch housing and its actuating arm is connected to the end of the clutch lever to apply the force and movement to actuate the clutch. Furthermore, an electronic control unit was used to apply the desired control inputs. The sampling time step size is 5 ms. Then, the simulation results were compared with the measurements on the test stand which has been done in the laboratory, as shown in Figs. 5 and 6. Some necessary modifications have been made in the model parameters, to get good agreements



with the test results. The diagram of angular position for electromotor shaft is plotted in Fig. 5 based on the results from the test bench. The motor current is illustrated in Fig. 6. The parameters of the electric motor model set according to the measurement results, are listed in Table 1. Some of these parameters have been obtained according to the test results of the electromotor dynamometer at laboratory and others have been determined by trial and error as well as performing several simulations and comparison of the simulation results with the experimental tests.

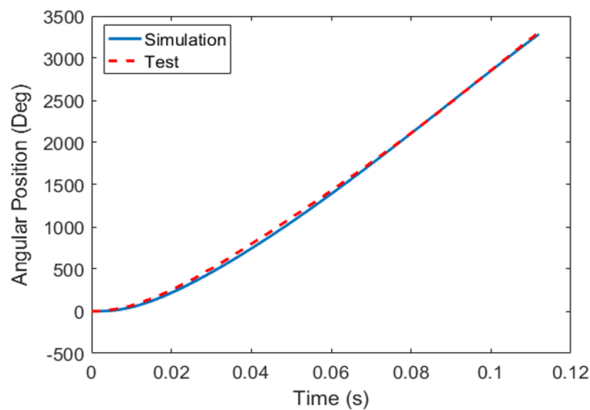


Fig. 5. Angular position of electromotor shaft

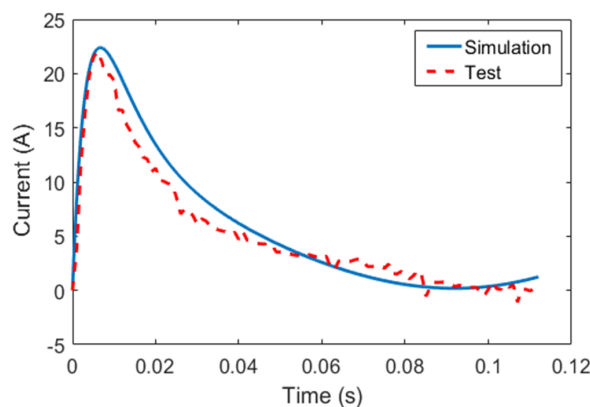


Fig. 6. The motor current

In both cases, very close agreement between test and simulation results was obtained after model updating. The simulation results of actuator model corresponding to the clutch bearing displacement and force of the clutch diaphragm spring are depicted in Figs. 7 and 8, respectively.

Table 1. Parameter values of the electric motor model

Parameter	Value
Armature inductance, $L_a$ (H)	$1.4 \times 10^{-3}$
Back electromotive force constant, $k_e$ (V s/rad)	0.0214
Viscous friction coefficient, $B_m$ (N m s/rad)	$5.7 \times 10^{-5}$
Armature resistance, $R$ ( $\Omega$ )	0.51
Moment of inertia, $J_m$ ( $\text{kg m}^2$ )	$1.2 \times 10^{-5}$
Electromechanical coupling coefficient, $k_t$ (N m/A)	0.0175
Input voltage of the motor, $u_a$ (V)	14

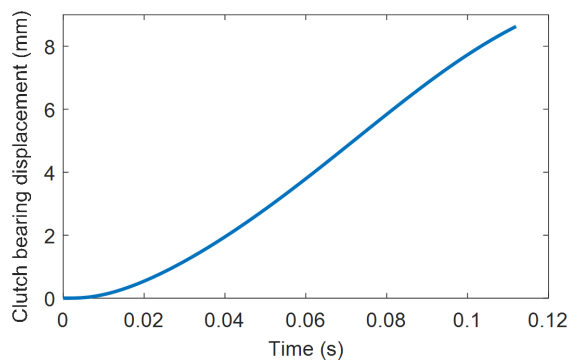


Fig. 7. The clutch bearing displacement

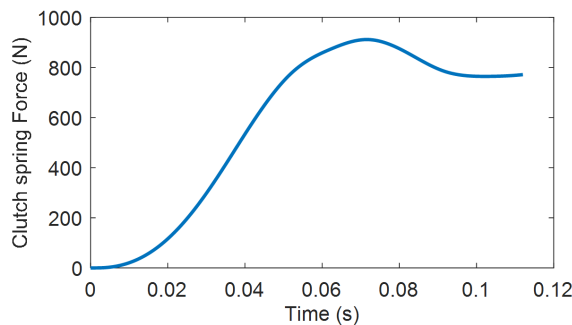


Fig. 8. The force of the clutch diaphragm spring

### 3. Estimation of state variables using the UKF

As mentioned earlier, the state variables are estimated based on the UKF. In this study, the state variables of angular velocity and angular acceleration of the gear, respectively  $\omega$  and  $\dot{\omega}$ , are estimated. It is noteworthy that the angular position of gear ( $\theta$ ) and motor current ( $i_a$ ) are the measurable variables.

To estimate the state variables utilizing the UKF, it is necessary to create a discrete-time non-linear state-space model based on the continuous-time model as follows:

$$x_{k+1} = f(x_{k+1}, u_k, t_k) + w_k \quad (14)$$

$$y_k = h(x_k, t_k) + v_k, \quad (15)$$

where  $f$  is the vehicle system dynamics,  $x_k$  is the state at the sampling instant  $k$ ,  $u_k$  is the input to the system at the sampling instant  $k$ ,  $y_k$  is a set of noisy measurements.  $w_k$  is the process noise, while  $v_k$  is the measurement noise. The added noises are assumed to be normally distributed Gaussian white noises with zero mean whose covariance matrices are  $Q$  and  $R$ , respectively [20].

#### 4. Design of the system controller

The controller design based on ASMC for automated clutch is presented in this section. First, the conventional SMC is introduced, and then the ASMC with adaptive gains is proposed. For the SMC, the error functions are defined by the following expression:

$$e_1 = x_c - x_d, \quad e_2 = v_c - v_d, \quad e_3 = a_c - a_d, \quad (16)$$

The sliding surface  $S$  consists of an integral component expressed as:

$$S = e_3 + k_1 e_2 + k_2 e_1 + k_3 \int_0^t e_1 dt, \quad (17)$$

where  $k_1$  and  $k_2$  are the strictly positive design scalars,  $x_d$ ,  $v_d$  and  $a_d$  are desired trajectory, velocity and acceleration,  $v_c$  and  $a_c$  are the values of clutch bearing velocity and acceleration obtained as

$$v_c = c_1 \omega, \quad a_c = c_1 \alpha. \quad (18)$$

By differentiating Eq. (17) and combining Eqs. (9), (10) and (18):

$$\begin{aligned} \dot{S} = \left( \frac{c_1}{I_a} \right) \left[ - \left( k_\omega + \frac{R_a I_a}{L_a} \right) \alpha - \left( \frac{R_a k_\omega + k_t N_m^2 k_e}{L_a} \right) \omega + \left( \frac{R_a T_L}{L_a} \right) + \dot{T}_L \right. \\ \left. + \left( \frac{k_t N_m}{L_a} \right) u_a \right] - \dot{a}_d + k_1 e_3 + k_2 e_2 + k_3 e_1. \end{aligned} \quad (19)$$

For the sliding surface to asymptotically approach zero, its dynamics should be considered as follows:

$$\dot{S} = -\eta \text{sign}(S) \quad (\eta > 0). \quad (20)$$

Consequently:

$$\frac{1}{2} \left( \frac{d}{dt} \right) S^2 = S\dot{S} = -\eta \operatorname{sign}(S)S < 0, \quad (21)$$

where  $\eta$  is a positive constant. According to Eqs. (16) to (19) and dynamic equations of system, the SMC control law can be described as:

$$u_a = \frac{L_a}{k_t N_m} \left[ \left( \frac{I_a}{c_1} \right) (\dot{a}_d - k_1 e_3 - k_2 e_2 - k_3 e_1 - \eta \operatorname{sign}(S)) + \left( k_\omega + \frac{R_a I_a}{L_a} \right) \alpha + \left( \frac{R_a k_\omega + k_t N_m^2 k_e}{L_a} \right) \omega - \hat{\lambda} T_L - \hat{\phi} \dot{T}_L \right] \quad (22)$$

in which  $\hat{\lambda} T_L$  is the estimated value of load torque for actuator,  $\lambda = \left( \frac{R_a}{L_a} \right)$ , and  $\hat{\phi} \dot{T}_L$  is estimated value of its derivative,  $\phi = 1$ . It is assumed the system uncertainties exist in the actuator torque and its derivative. This chattering may increase highly control effort and excite un-modelled high-frequency dynamics, as well. So, to mitigate this problem, the sign function is replaced by the saturation function  $\operatorname{sat}(S/\psi)$  with a boundary layer thickness of  $\psi > 0$ . The control input voltage applied to the actuator electromotor has the following condition imposed:

$$u_a = \begin{cases} -14 & u_a \leq -14, \\ u_a & -14 < u_a < 14, \\ 14 & u_a \geq 14. \end{cases} \quad (23)$$

Now the stability of the proposed SMC system is proved. First, the function  $d(t)$  is defined as the disturbance load in the actuator dynamics. This is because of un-modelled dynamics and uncertainties in modelling the actual nonlinear dynamics of actuator and diaphragm clutch.

$$d(t) = \frac{c_1(\tilde{\lambda} T_L + \tilde{\phi} \dot{T}_L)}{I_a} \quad (24)$$

in which  $\tilde{\lambda}$  is the difference between the estimated value  $\hat{\lambda}$  and the actual value  $\lambda$ . So,  $\tilde{\lambda} = \hat{\lambda} - \lambda$ . Similarly, the difference between the estimated and actual values of  $\phi$  is defined as  $\tilde{\phi} = \hat{\phi} - \phi$ . The term  $d(t)$  is assumed to be bounded by following equation:

$$|d(t)| < \eta. \quad (25)$$

As a result, the system uncertainties and disturbances are bounded. The candidate Lyapunov function is defined as:

$$V = \frac{1}{2} \lambda S^2 + \frac{1}{2} \phi S^2. \quad (26)$$

Using Eqs. (19) and (22) and expression  $S \operatorname{sign}(S) = |S|$ , the time derivative of the scalar  $V$  is calculated as:

$$\begin{aligned} \dot{V} &= (\lambda + 1)S \left( \frac{c_1 (\tilde{\lambda}T_L + \tilde{\phi}\dot{T}_L)}{I_a} - \eta \operatorname{sign}(S) \right) \\ &= (\lambda + 1)S (d(t) - \eta \operatorname{sign}(S)) \\ &= (\lambda + 1) (Sd(t) - \eta |S|) \leq (\lambda + 1) (|S| |d(t)| - \eta |S|) \\ &\leq (\lambda + 1) |S| (|d(t)| - \eta). \end{aligned} \quad (27)$$

It can be concluded from Eq. (25):

$$\dot{V} < 0. \quad (28)$$

Since the function  $V$  is positive definite and  $\dot{V}$  is negative definite, therefore, it can be concluded according to the Barbalat's Lemma that the designed control system is stable and the sliding surface  $S$  tends to zero asymptotically. The overall structure of the proposed controller scheme for clutch actuator is shown in Fig. 9.

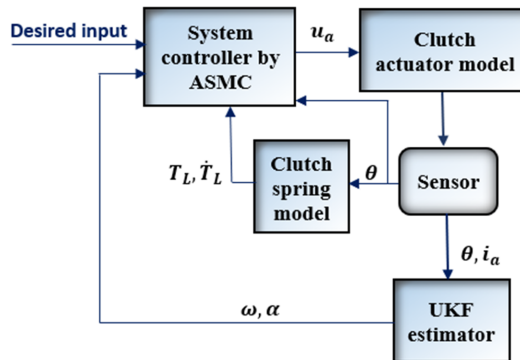


Fig. 9. Overall structure of the proposed controller scheme

The SMC gains  $k_1, k_2, k_3$  and  $\eta$  depend on the upper bounds of uncertainties in the actuator clutch controller such as the load torque of actuator and its derivative. These gains should be tuned by a trial-and-error method in the practical applications. To overcome this disadvantage, the sliding mode control with adaptive gains has been presented. Accordingly, the Eq. (20) is modified as:

$$\dot{S} = -\eta(t) \operatorname{sat}(S/\psi). \quad (29)$$

The varying controller gains are updated by the following expressions:

$$\dot{\eta}(t) = \eta_0 |S|, \quad (\eta_0 = 300), \quad (30)$$

$$\dot{k}_1 = k_{1,0} |S|, \quad (k_{1,0} = 520), \quad (31)$$

$$\dot{k}_2 = k_{2,0} |S|, \quad (k_{2,0} = 55000), \quad (32)$$

$$\dot{k}_3 = k_{3,0} |S|, \quad (k_{3,0} = 1300). \quad (33)$$

## 5. Simulation results and discussion

In this part, first, the accuracy of proposed SMC combined with the UKF estimator is evaluated without any torque disturbance for the model with nominal parameters. Then, the high effectiveness of the proposed ASMC is demonstrated against the conventional SMC to track precisely the desired trajectories with uncertainties in modelling the clutch spring torque. The objective is to control the clutch to move from the initial position to the end. Hence, the position control of clutch can be analyzed in this investigation by adopting the SMC controller and ASMC.

The clutch displacement tracking performance of the AMT is chosen as the typical operating condition to validate the designed SMC, which is obtained from the experimental data and is given by:

$$x_d = \begin{cases} 0 & t \leq 0.2, \\ 4.583t + 0.583 & 0.2 < t < 1.4, \\ 8 & t \geq 1.4. \end{cases} \quad (34)$$

The unit of  $x_d$  is mm. It is supposed that the gains of SMC are  $k_1 = 80$ ,  $k_2 = 1700$ ,  $k_3 = 400$ ,  $\eta = 300$ , and  $\psi = 0.5$ . The dynamic response obtained by using the SMC, is depicted in Fig. 10. A preferable tracking response can be seen. The actual trajectory response of the presented controller approaches the desired path  $x_d(t)$  rapidly, as shown in Fig. 10. The corresponding tracking error is illustrated in Fig. 11.

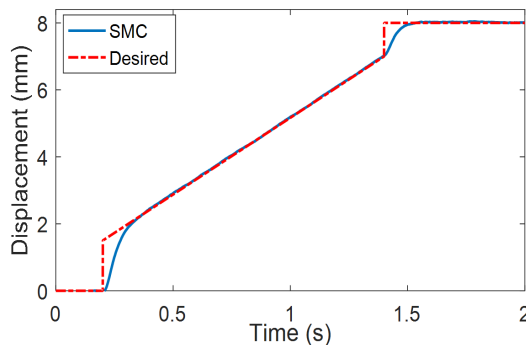


Fig. 10. Clutch bearing displacement tracking performance using SMC

According to Fig. 11, it can be observed that the steady state tracking error of clutch bearing displacement is very small and nearly neglectable. Its magnitude is about 0.01 mm. Fig. 12 shows the input voltage applied to the actuator electromotor. The angular position of actuator gear is plotted in Fig. 13. By comparison with Figs. 13 and 10, it can be realized that the relationship among the clutch bearing displacement and angular position is linear, as expressed in Eq. (6). Fig. 14 illustrates the current passing the electric circuit. Fig. 15 gives the simulation results

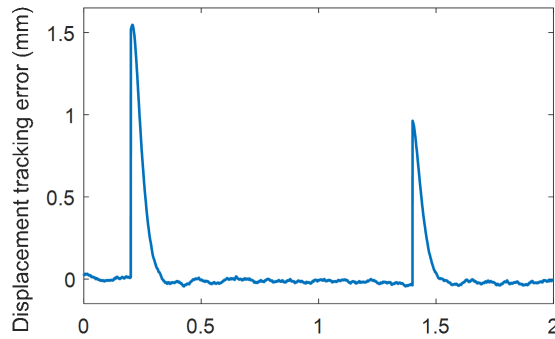


Fig. 11. Tracking error of clutch bearing displacement using SMC

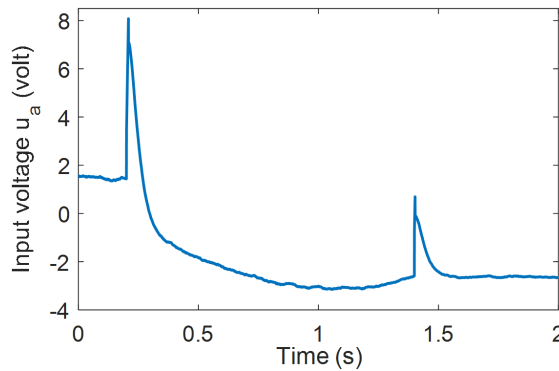


Fig. 12. Control input voltage

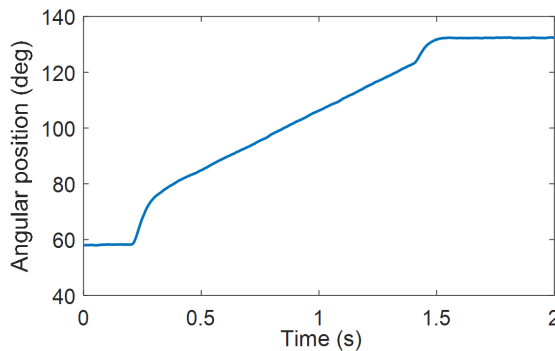


Fig. 13. Angular position of actuator gear

of the angular velocity for actuator gear with the UKF estimator (Estimated), and without estimator (Actual value). In addition, the angular acceleration of actuator gear is depicted in Fig. 16. According to the simulation results, it can be found that the estimated values using the proposed UKF is perfectly precise and reliable without a noticeable error. However, the estimated results deviate rarely far away from

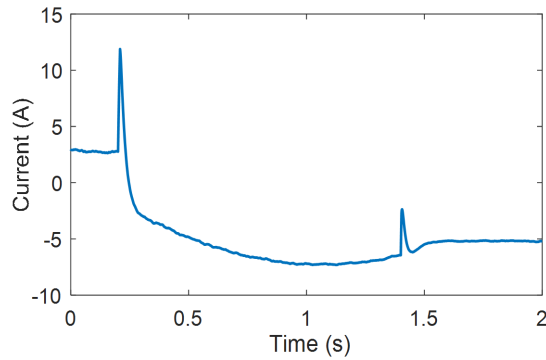


Fig. 14. The current passing the electric circuit

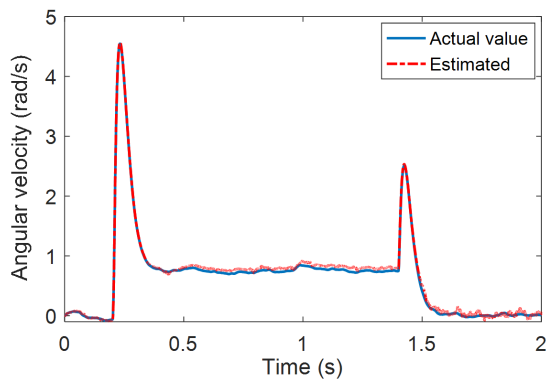


Fig. 15. The angular velocity of actuator gear

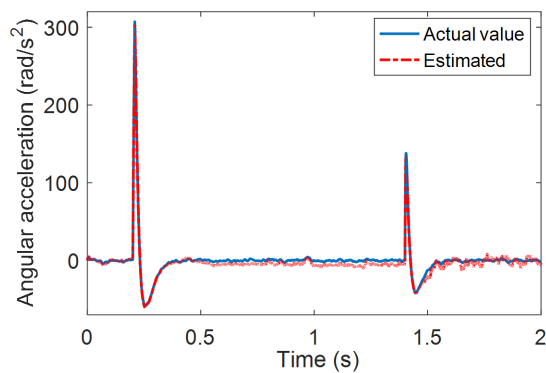


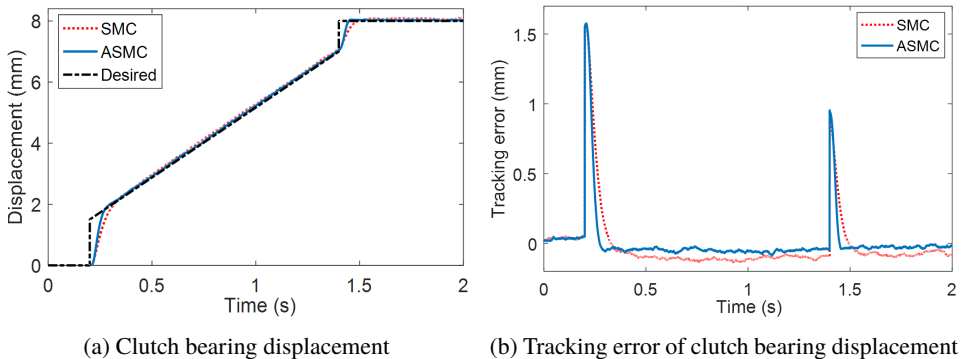
Fig. 16. The angular acceleration of actuator gear

the actual values when the system response is transient and not steady state. The main reason can be due to inadequate excitation. Overall, the estimation accuracy is greatly demonstrated and the UKF estimator can be effective.



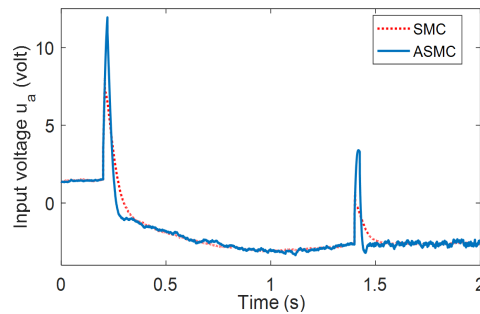
According to the simulation results, it is clear, that the designed SMC combined with the UKF estimator is efficient to track precisely the desired trajectories for the clutch displacement.

However, the proposed SMC system cannot perform with high accuracy in the presence of parameter uncertainties and external disturbance. Since the transmission systems undergo changes in parameters with respect to the wide range of driving condition, such as changing in friction coefficient of clutch disc and stiffness of diaphragm spring, and the longer-time wear and tear during the running period, an ASMC method is required to guarantee good tracking performance and cope with the uncertainties and disturbances. To achieve this, in the following, the simulations are conducted under two different conditions of parameter uncertainties in modelling for load torque of clutch spring. Let us assume that parameters of the Eq. (8) have been decreased 10% firstly, then 20%. In order to assess the performance of proposed adaptive controller, the results of the ASMC are compared with the SMC. The simulation results are seen in Fig. 17 corresponding to reduction of 10% in the mentioned parameters. The clutch displacement, tracking error of clutch bearing displacement, and the input voltage are plotted in Figs. 17a,



(a) Clutch bearing displacement

(b) Tracking error of clutch bearing displacement



(c) Control input voltage

Fig. 17. Evaluation of SMC performance in comparison with the ASMC in the presence of 10% parameter uncertainties

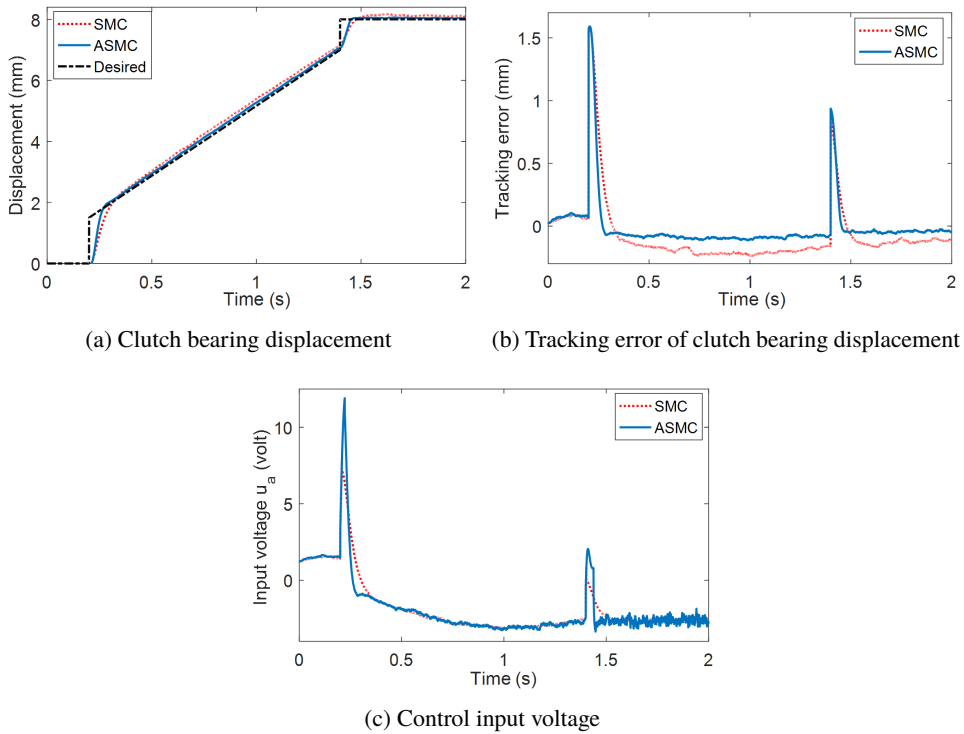


Fig. 18. Evaluation of SMC performance in comparison with the ASMC in the presence of 20% parameter uncertainties

17b and 17c, respectively. In the same way, the analysis results are illustrated in Fig. 18 corresponding to reduction of 20% in the mentioned parameters.

An important index for the better quantitative evaluation of the proposed control systems is the root mean square (RMS) value of the tracking error of clutch position defined as:

$$\text{RMS}(e_1) = \sqrt{\frac{1}{T} \int_0^T e_1^2 dt}. \quad (35)$$

The RMS values of tracking error for the control systems are computed, as given in Table 2.

Table 2. Comparison between the RMS of tracking error for different control systems

Parameter uncertainties	10%		20%	
Control system	SMC	ASMC	SMC	ASMC
RMS of error (mm)	0.251	0.216	0.282	0.225
Relative improvement of ASMC	14%		20%	

The results demonstrate the high effectiveness of the proposed ASMC controller against the traditional SMC to track the desired trajectories. Also, the state variables of the system have been precisely estimated using UKF without a considerable error.

## 6. Conclusions

This paper proposed an ASMC combined with the UKF estimator for the automated clutch system. The stability of the controller was approved by using the Lyapunov theorem and the robustness of the designed ASMC was investigated by performing some computer simulations based on a validated non-linear model for clutch actuator. The analyses are conducted under two different conditions of parameter uncertainties. It was presumed that the parameters of the clutch spring model were decreased 10% and 20%. A precise tracking response of position control can be observed by employing the proposed ASMC in the presence of parameter uncertainties against the traditional SMC. Also, the UKF was applied to estimate precisely the full states of system without a significant error. The contributions of this study are the following:

The first contribution of this paper is to build a validated model for the electromechanical clutch actuator with unknown dynamic model and parameters. By comparison with the test results and simulation analyses, the actuator model was verified. The second, is that a nonlinear estimator was proposed through UKF to estimate the variables that cannot be measured in a cost-efficient way, such as rotational speed and angular acceleration. The third one, is presenting the high effectiveness of the ASMC against the conventional SMC to track exactly the reference trajectories and control the dynamic systems accompanied by uncertainties and disturbances.

## Acknowledgements

The authors are very grateful to the Research and Development group of NiroMoharreke industrial (NMI) company for technical support.

## References

- [1] J. Horn, J. Bamberger, P. Michau, and S. Pindl. Flatness-based clutch control for automated manual transmissions. *Control Engineering Practice*, 11(12):1353–1359, 2003. doi: [10.1016/S0967-0661\(03\)00099-6](https://doi.org/10.1016/S0967-0661(03)00099-6).
- [2] L. Glielmo, L. Iannelli, V. Vacca, and F. Vasca. Gearshift control for automated manual transmissions. *IEEE/ASME Transactions on Mechatronics*, 11(1):17–26, 2006. doi: [10.1109/TMECH.2005.863369](https://doi.org/10.1109/TMECH.2005.863369).
- [3] Z. Zhong, G. Kong, Z. Yu, X. Chen, X. Chen, and X. Xin. Concept evaluation of a novel gear selector for automated manual transmissions. *Mechanical Systems and Signal Processing*, 31:316–331, 2012. doi: [10.1016/j.ymssp.2012.02.008](https://doi.org/10.1016/j.ymssp.2012.02.008).

- [4] Y. Zhao, Z. Liu, L. Cai, W. Yang, J. Yang, and Z. Luo. Study of control for the automated clutch of an automated manual transmission vehicle based on rapid control prototyping. *Proceedings of the Institution of Mechanical Engineers, Part D: Journal of Automobile Engineering*, 224(4):475–487, 2010. doi: [10.1243/09544070JAUTO1245](https://doi.org/10.1243/09544070JAUTO1245).
- [5] X. Song, Z. Sun, X. Yang, and G. Zhu. Modelling, control, and hardware-in-the-loop simulation of an automated manual transmission. *Proceedings of the Institution of Mechanical Engineers, Part D: Journal of Automobile Engineering*, 224(2):143–160, 2010. doi: [10.1243/09544070JAUTO1284](https://doi.org/10.1243/09544070JAUTO1284).
- [6] S. Lin, S. Chang, and B. Li. Improving the gearshifts events in automated manual transmission by using an electromagnetic actuator. *Proceedings of the Institution of Mechanical Engineers, Part C: Journal of Mechanical Engineering Science*, 229(9):1548–1561, 2015. doi: [10.1177/0954406214546204](https://doi.org/10.1177/0954406214546204).
- [7] Z. Chen, B. Zhang, N. Zhang, H. Du G. Kong. Optimal preview position control for shifting actuators of automated manual transmission. *Proceedings of the Institution of Mechanical Engineers, Part D: Journal of Automobile Engineering*, 233(2):440–452, 2019. doi: [10.1177/0954407017745981](https://doi.org/10.1177/0954407017745981).
- [8] C.Y. Tseng and C.H. Yu. Advanced shifting control of synchronizer mechanisms for clutchless automatic manual transmission in an electric vehicle. *Mechanism and Machine Theory*, 84:37–56, 2015. doi: [10.1016/j.mechmachtheory.2014.10.007](https://doi.org/10.1016/j.mechmachtheory.2014.10.007).
- [9] G. Kong, N. Zhang, and B. Zhang. Novel hybrid optimal algorithm development for DC motor of automated manual transmission. *International Journal of Automotive Technology*, 17(1):135–143, 2016. doi: [10.1007/s12239-016-0013-1](https://doi.org/10.1007/s12239-016-0013-1).
- [10] J. Oh, J. Kim, and S. Choi. Robust feedback tracking controller design for self-energizing clutch actuator of automated manual transmission. *SAE International Journal of Passenger Cars-Mechanical Systems*, 6(3):1510–1517, 2013. doi: [10.4271/2013-01-2587](https://doi.org/10.4271/2013-01-2587).
- [11] A. Bagheri, S. Azadi, and A. Soltani. A combined use of adaptive sliding mode control and unscented Kalman filter estimator to improve vehicle yaw stability. *Proceedings of the Institution of Mechanical Engineers, Part K: Journal of Multi-body Dynamics*, 231(2):388–401, 2017. doi: [10.1177/1464419316673960](https://doi.org/10.1177/1464419316673960).
- [12] B. Gao, Y. Lei, A. Ge, H. Chen, and K. Sanada. Observer-based clutch disengagement control during gear shift process of automated manual transmission. *Vehicle System Dynamics*, 49(5):685–701, 2011. doi: [10.1080/00423111003681354](https://doi.org/10.1080/00423111003681354).
- [13] R. Temporelli, M. Boisvert, P. Micheau. Control of an electromechanical clutch actuator using a dual sliding mode controller: Theory and experimental investigations. *IEEE/ASME Transactions on Mechatronics*, 24(4):1674–1685, 2019. doi: [10.1109/TMECH.2019.2919673](https://doi.org/10.1109/TMECH.2019.2919673).
- [14] S.A. Haggag. Sliding mode adaptive PID control of an automotive clutch-by-wire actuator. *SAE International Journal of Passenger Cars-Mechanical Systems*, 9(1):424–433, 2016. doi: [10.4271/2016-01-9106](https://doi.org/10.4271/2016-01-9106).
- [15] J. Park and S. Choi. Optimization method of reference slip speed in clutch slip engagement in vehicle powertrain. *International Journal of Automotive Technology*, 22:55–67, 2021. doi: [10.1007/s12239-021-0007-5](https://doi.org/10.1007/s12239-021-0007-5).
- [16] Z. Sun, B. Gao, J. Jin, and K. Sanada. Modelling, analysis and simulation of a novel automated manual transmission with gearshift assistant mechanism. *International Journal of Automotive Technology*, 20:885–895, 2019. doi: [10.1007/s12239-019-0082-z](https://doi.org/10.1007/s12239-019-0082-z).
- [17] G. Xia, J. Chen, X. Tang, L. Zhao, and B. Sun. Shift quality optimization control of power shift transmission based on particle swarm optimization–genetic algorithm. *Proceedings of the Institution of Mechanical Engineers, Part D: Journal of Automobile Engineering*, 236(5):872–892, 2022. doi: [10.1007/s12239-019-0082-z](https://doi.org/10.1007/s12239-019-0082-z).

- [18] M. Sharifzadeh, M. Pisaturo, and A. Senatore. Real-time identification of dry-clutch frictional torque in automated transmissions at launch condition. *Proceedings of the Institution of Mechanical Engineers, Part D: Journal of Automobile Engineering*, 234(2-3):586–598, 2020. doi: [10.1177/0954407019857268](https://doi.org/10.1177/0954407019857268).
- [19] X. Zhu, H. Zhang, J. Xi, J. Wang, and Z. Fang. Robust speed synchronization control for clutchless automated manual transmission systems in electric vehicles. *Proceedings of the Institution of Mechanical Engineers, Part D: Journal of Automobile Engineering*, 229(4):424–436, 2015. doi: [10.1177/0954407014546431](https://doi.org/10.1177/0954407014546431).
- [20] H. Ren, S. Chen, T. Shim, and Z. Wu. Effective assessment of tyre–road friction coefficient using a hybrid estimator. *Vehicle System Dynamics*, 52(8):1047–1065, 2014. doi: [10.1080/00423114.2014.918629](https://doi.org/10.1080/00423114.2014.918629).